Available online at www.sciencedirect.com
SCIENCE DIRECT®
Journal of Non-Crystalline Solids 338–340 (2004) 322–325
JOURNAL OF NON-CRYSTALLINE SOLIDS
www.elsevier.com/locate/jnoncrysol

Determination of the density of defect states by thermally stimulated conductivity studied from numerical simulations

J.A. Schmidt *, R.R. Koropecki, R. Arce, A. Dussan, R.H. Buitrago

INTEC (CONICET – UNL), Güemes 3450, 3000 Santa Fe, Argentina

Available online 1 April 2004

Abstract

Starting from the multiple trapping rate equations that define the non-equilibrium concentrations of electrons and holes in extended states, the thermally stimulated conductivity (TSC) experiment is examined. A system of non-linear coupled differential equations is solved to get the temporal evolution of the occupation functions and the carrier concentrations during the initial isothermal waiting time and the subsequent heating at a constant rate. The simulated TSC spectra reproduce the reported dependence of the measured spectra on the heating rate and the starting temperature. An approximate expression to obtain the DOS distribution in the upper half of the band gap from TSC spectra is deduced. The application of this expression to simulated TSC curves provides an accurate reconstruction of the introduced DOS. The TSC method compares favourably to the modulated photoconductivity experiments, both from the quality of the DOS reconstruction and the experimental simplicity of the method.

PACS: 72.20.Jv; 71.23.–k

1. Introduction

In the thermally stimulated conductivity (TSC) technique a sample is cooled down to a temperature T_0, illuminated for a time t_{ill}, and after a delay period t_d, heated in the dark at a constant rate β. The experimental simplicity of the technique has made it an appealing choice to measure the density of trap states in semiconductors. Assuming quasi-equilibrium conditions and considering that electron emission is the relevant process that rules the TSC, a simple expression yielding the DOS from a TSC spectrum can be easily obtained [1]. However, doubts have arisen about the underlying processes that give rise to the TSC [2], while recent simulations have thrown doubt about the possibility to correlate a TSC curve to the DOS structure [3].

Simmons et al. [4] provided the first consistent theory of the TSC in a system having a continuous trap distribution, assuming thermal equilibrium and neglecting recombination. Fritzsche and Ibaraki [5] developed a theory of the TSC taking recombination into account, but neglecting retrapping. Gu et al. [6] were the first to base their analysis on the multiple trapping model, taking into account thermal emission, trapping and recombination processes. However, they approximated the occupation functions by Fermi functions and they restricted their analysis to electrons only. Baranovskii et al. [7] extended the theoretical model to low temperatures, including transport via hopping of carriers through the localised band-tail states. More recently, Smaïl et al. [3] solved for the first time the complete set of differential equations, taking into account all the relevant transitions both for electrons and holes. These authors, however, restricted their analysis to midgap defects having a delta-like distribution. Based on numerical calculations, they concluded that it is difficult to correlate a TSC curve to the DOS structure.

In this work we present numerical simulations of light-induced TSC and steady-state photoconductivity experiments, which are combined to obtain the DOS in the upper half of the band gap. An expression that provides the DOS from TSC spectra is deduced and tested through simulations.

* Corresponding author. Tel.: +54-342 4559175; fax: +54-342 4550944.
E-mail address: jschmidt@intec.unl.edu.ar (J.A. Schmidt).

0022-3093/$ - see front matter © 2004 Elsevier B.V. All rights reserved.
doi:10.1016/j.jnoncrysol.2004.02.065

2. Simulation details

The DOS used as a starting point for our simulations consists of exponential band tails of monovalent states, and defect states with Gaussian distributions, considered to be either monovalent or amphoteric. In this later case, we consider dangling bond states with three possible charge states, D^+, D^0 and D^-, and a positive correlation energy U.

After illumination, the concentration of excess carriers in extended states arises from a balance between thermal emission, capture and recombination. The rate equations governing the concentration of electrons $n(t)$ and holes $p(t)$ in the extended states, and the occupation functions f, f^+, f^0 and f^- (for monovalent, positively charged, neutral and negatively charged defects, respectively) are the following:

$$\begin{aligned}
\frac{\partial n}{\partial t} &= \int_{E_v}^{E_c} [e_n f - c_n n(1-f)] D^M \, dE \\
&\quad + \int_{E_v}^{E_c} [e_n^0 f^0 + e_n^- f^- - c_n^0 n f^0 - c_n^+ n f^+] D^{DB} \, dE, \\
\frac{\partial p}{\partial t} &= \int_{E_v}^{E_c} [e_p(1-f) - c_p p f] D^M \, dE \\
&\quad + \int_{E_v}^{E_c} [e_p^0 f^0 + e_p^+ f^+ - c_p^0 n f^0 - c_p^- n f^-] D^{DB} \, dE, \\
\frac{\partial f}{\partial t} &= c_n n(1-f) + e_p(1-f) - e_n f - c_p p f, \\
\frac{\partial f^+}{\partial t} &= e_n^0 f^0 + c_p^0 p f^0 - e_p^+ f^+ - c_n^+ n f^+, \\
\frac{\partial f^0}{\partial t} &= -\frac{\partial f^+}{\partial t} - \frac{\partial f^-}{\partial t}, \\
\frac{\partial f^-}{\partial t} &= e_p^0 f^0 + c_n^0 n f^0 - e_n^- f^- - c_p^- p f^-,
\end{aligned} \tag{1}$$

where t is the time variable, E_v and E_c are the energies at the top of the valence band and the bottom of the conduction band, respectively, D^M is the density of monovalent defects, D^{DB} is the density of dangling bonds, e represents the thermal emission coefficient, and c the capture coefficient; subscripts (n or p) indicate that the coefficient is for electrons or holes, and superscripts $(+, 0, -)$ indicate that the coefficient is for positively charged, neutral or negatively charged DB (no superscript indicates that the coefficient is for monovalent traps). The time and/or energy dependence of the functions is not indicated for the sake of clarity.

By using numerical methods we solve the set of nonlinear differential equations to get $n(t)$ and $p(t)$ (or, equivalently, $n(T)$ and $p(T)$ since temperature depends linearly on time, $T(t) = T_0 + \beta t$). The TSC spectrum is obtained from

$$\sigma_{TSC}(T) = [q\mu_n n(T) + q\mu_p p(T)] - \sigma_{dk}(T), \tag{2}$$

where q is the electronic charge, and μ_n, μ_p are the electron and hole mobilities in extended states, respectively. The dark conductivity as a function of temperature, $\sigma_{dk}(T)$, is calculated independently by solving the charge neutrality equation for each temperature. The initial decay of the conductivity during the waiting time t_d is also calculated from the same rate equations.

3. Results and discussion

Due to length limitations we will restrict our analysis to the case of monovalent defects and to samples where electrons dominate the conductivity. Setting $D^{DB} \equiv 0$ in Eq. (1), and dropping the superscript for the monovalent defects, we have

$$\frac{\partial n(T)}{\partial t} = \int_{E_v}^{E_c} e_n f D \, dE - n(T) \int_{E_v}^{E_c} c_n (1-f) D \, dE, \tag{3}$$

$$\frac{\partial p(T)}{\partial t} = \int_{E_v}^{E_c} e_p (1-f) D \, dE - p(T) \int_{E_v}^{E_c} c_p f D \, dE. \tag{4}$$

From the exact solutions $n(T)$ and $p(T)$ we have checked the quasi-equilibrium conditions, $\frac{\partial n}{\partial t} \cong 0$, $\frac{\partial p}{\partial t} \cong 0$. Thus, from Eq. (3) we can write

$$n(T) = \int_{E_v}^{E_c} e_n f D \, dE \Big/ \int_{E_v}^{E_c} c_n (1-f) D \, dE. \tag{5}$$

The function $e_n(E,T) \times f(E,T)$ is a peaked function with a sharp maximum at an energy $E_m(T)$. This energy is independent on the DOS, and varies linearly with temperature. At each temperature, we have numerically found the energy for which the function is maximum. The examination of a large number of cases led us to the following dependence:

$$E_c - E_m(T) = C_1(T_0) \times k_s T \times \ln[C_2(T_0)\nu/\beta] - C_3(T_0), \tag{6}$$

where k_B is Boltzmann's constant, ν is the attempt-to-escape frequency, and the coefficients C_i depend on the initial temperature T_0 as: $C_1(T_0) = 0.9762 - 7.429 \times 10^{-5} T_0$, $C_2(T_0) = 15.58 + 0.3379 T_0$, $C_3(T_0) = 0.00773 + 8.873 \times 10^{-5} T_0$. These expressions have been obtained in the range $30\ \text{K} < T_0 < 140\ \text{K}$. In Eq. (6), energies are expressed in eV, ν in s^{-1} and β in K/s.

The sharply peaked function $e_n(E,T) \times f(E,T)$ can be replaced by a δ-like function centered at E_m, with a weighting factor $W(T)$. On the other hand, the factor $\left[\int_{E_v}^{E_c} c_n(1-f) D \, dE\right]^{-1}$, which represents the density of unoccupied capture centres, can be associated to the electron lifetime, τ_n [8]. Thus, we finally obtain

$$\begin{aligned}
n(T) &= \tau_n \times \int_{E_v}^{E_c} W(T) \delta(E - E_m) D(E) \, dE \\
&= \tau_n \times W(T) \times D(E_m).
\end{aligned}$$

For the function $W(T)$ we have found $W(T) = \beta[0.97k_B \ln(\nu T/\beta) - 7.33 \times 10^{-5}]$. If electrons dominate the conductivity, the DOS at the peak energy $E_m(T)$ is given by

$$D(E_m) = \frac{\sigma_{TSC}(T)}{q\mu_n\tau_n W(T)}, \quad (7)$$

where $\sigma_{TSC}(T)$ can be measured in the TSC experiment, and the $\mu_n \times \tau_n$ product can be obtained from the steady state photoconductivity as already described by Zhu and Fritzsche [9].

By using this formula we have reconstructed the DOS characterised by the parameters listed in Table 1. These parameters are quite typical for a–Si:H, except for the attempt-to-escape frequency which was taken as $\nu = 5 \times 10^9$ s^{-1} to reproduce the typically measured temperature at which $\sigma_{TSC}(T)$ drops to zero. Different values for the attempt-to-escape frequency of a–Si:H have been reported in the literature [1,5,9]. We have performed calculations for a starting temperature 20 K $\leqslant T_0 \leqslant$ 100 K, a heating rate 0.025 K/s $\leqslant \beta \leqslant$ 0.075 K/s, and an illumination generation rate $G = 3.2 \times 10^{19}$ cm^{-3} s^{-1}. The waiting period in dark before heating was $t_d = 300$ s in all cases. The simulated TSC curves can be seen in Fig. 1. The general shape of experimental spectra is well reproduced, with a low temperature peak located around 90 K and a high temperature peak around 300 K.

The dependence of the TSC spectra on the heating rate β is a stringent test for the models that describe the TSC. In Fig. 1 we present a set of simulated spectra for $T_0 = 80$ K and different values of β. As it can be seen in the inset of Fig. 1, the peak moves to higher temperatures and increases in height, in agreement with measurements from Baranovskii et al. [7] and Misra et al. [10]. Fig. 2 shows the DOS reconstructions performed from this set of TSC spectra. As it can be seen, the reconstructions agree within each other, and reproduce quite accurately the introduced DOS.

Table 1
Parameters used in the numerical simulations

Parameter	Value
E_v (energy at the valence band top)	0
E_c (energy at the conduction band bottom)	1.8 eV
$N(E_c) = N(E_v)$ (DOS at the band edges)	10^{21} cm^{-3} eV^{-1}
E_{vt} (valence band tail characteristic energy)	56 meV
E_{ct} (conduction band tail characteristic energy)	28 meV
DB (total density of defects, acceptors + donors)	2×10^{16} cm^{-3}
C_d (centre of the Gaussian distribution, donors)	0.85 eV
C_a (centre of the Gaussian distribution, acceptors)	1.25 eV
w_d (width of the Gaussian distributions)	0.2 eV
ν (attempt-to-escape frequency)	5×10^9 s^{-1}
μ_n (free electron mobility)	10 cm^2 V^{-1} s^{-1}
μ_p (free hole mobility)	1 cm^2 V^{-1} s^{-1}

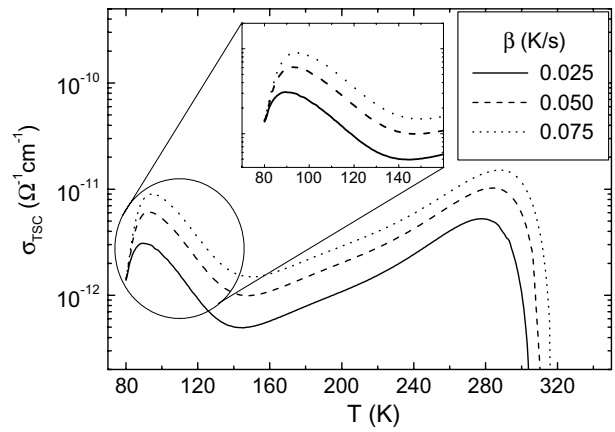

Fig. 1. Simulated TSC spectra for different heating rates (β). The shift of the low temperature peak and its change in height as a function of β can be observed in detail in the inset.

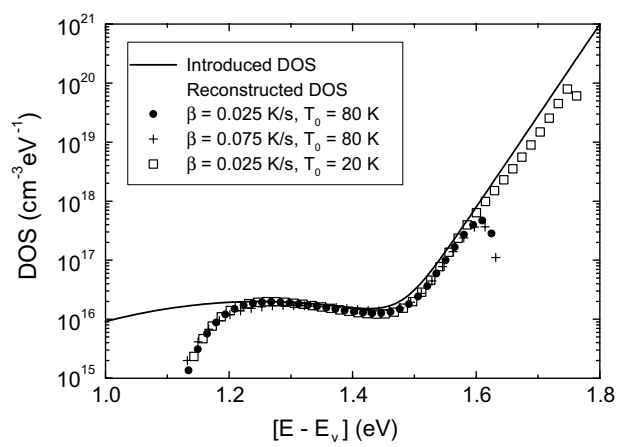

Fig. 2. Reconstruction of the introduced DOS from the simulated TSC spectra of Fig. 1. Different symbols correspond to different heating rates and starting temperatures T_0 as indicated in the inset.

Another test for a model that attempts to describe the TSC is to perform experiments at different starting temperatures T_0. Baranovskii et al. [7], and Zhou and Elliot [2] have found that there is a certain starting temperature T_0^* below which the position of the low-temperature TSC peak, T_m, does not change. Depending on the heating rate and the sample, this temperature T_m^* lies between 60 and 110 K. It has been suggested [7] that this behaviour, characteristic of the low temperature portion of the TSC spectra, may be explained in terms of conduction by hopping. As it can be seen in Fig. 3, this behaviour is reproduced by the rate equations that we are using although we do not include in our model hopping conductivity. The temperature T_0^* seems to be around 60 K in this case. In Fig. 2 we have already presented the DOS reconstruction from the TSC curve starting at $T_0 = 20$ K. As it can be observed, the DOS can now be reconstructed over a wider energy range. The curve agrees perfectly well with those obtained at

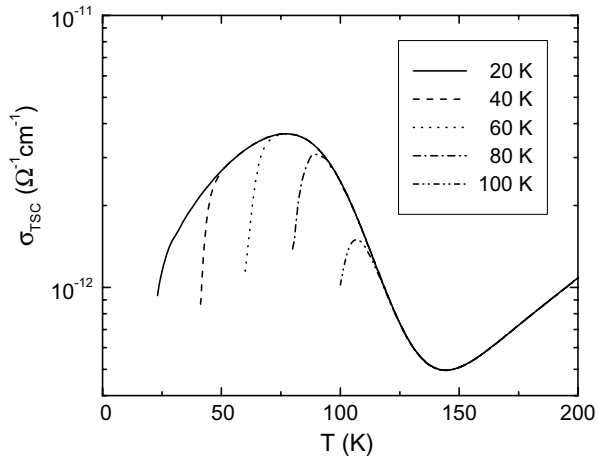

Fig. 3. Low temperature behaviour of the TSC spectra for different starting temperatures T_0 as indicated in the inset.

the starting temperature $T_0 = 80$ K, while it reproduces the introduced DOS quite accurately. A slight energy shift in the conduction band tail can be observed, but the slope is accurate within 6%. Thus, the simple formula given in Eq. (7) provides an accurate reconstruction of the DOS, provided the correct values of the initial temperature T_0 and the heating rate β are introduced in the expressions for $E_m(T)$ and $W(T)$.

It has been shown in previous works that the modulated photoconductivity (MPC) methods can be used to reproduce the DOS in the upper half of the band gap [11,12]. Starting from the same DOS distribution presented in Fig. 2, we have simulated the application of the MPC methods to reconstruct the DOS. The conventional MPC (c-MPC) technique has been simulated with a dc generation rate $G_{dc} = 10^{15}$ cm^{-3} s^{-1}, while the recombination regime MPC (RRMPC) has been simulated with $G_{dc} = 3.2 \times 10^{19}$ cm^{-3} s^{-1}. In both cases we have taken the ac component to be $G_{ac} = G_{dc}/20$. The comparison between the three methods is presented in Fig. 4. As it can be seen, the TSC reconstruction is more accurate in this case, and the DOS can be obtained over a wider energy range. From the experimental point of view, the three methods require to perform measurements as a function of temperature, but TSC has the advantage that it is not needed to use ac illumination, and only dc magnitudes are measured.

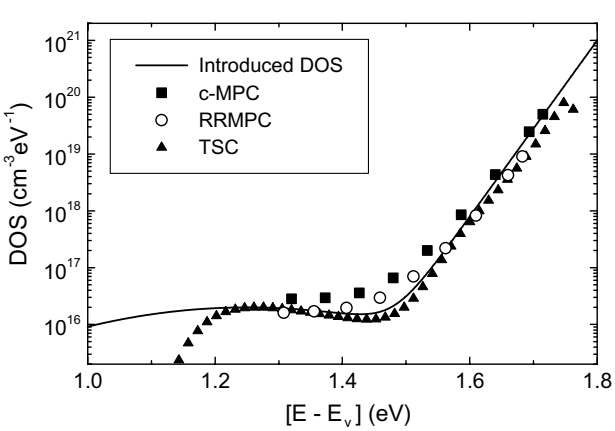

Fig. 4. Comparison of the DOS reconstructions obtained form simulated experiments of TSC and modulated photoconductivity in the trapping regime (c-MPC) and the recombination regime (RRMPC).

4. Conclusion

A consistent numerical calculation of TSC spectra taking into account all the relevant capture and emission processes for electrons and holes is presented. Starting from a realistic DOS distribution, we simulate the TSC spectra and we apply the same procedure that is used experimentally to reconstruct the defect density. Contrary to what it was concluded in some previous works, our simulations reveal that the TSC method provides a simple an accurate method to obtain the DOS distribution in the upper half of the gap of intrinsic a–Si:H. The TSC experiment compares favourably with the modulated photoconductivity experiments, both from the quality of the DOS reconstruction and from the experimental simplicity of the method.

Acknowledgements

This work was partially supported with grants of ANPCyT (PICT 12-06950) and CAI+D 2000-84-6-1. J.A.S. acknowledges support from the Alexander von Humboldt foundation and the Fundación Antorchas.

References

[1] G. Landweer, J. Bezemer, in: H. Fritzsche (Ed.), Amorphous Silicon and Related Materials, World Scientific, Singapore, 1988, p. 525.
[2] J.-H. Zhou, S.R. Elliot, Phys. Rev. B 46 (1992) 9792.
[3] T. Smaïl, M. Aoucher, T. Mohammed-Brahim, J. Non-Cryst. Solids 266–269 (2000) 376.
[4] J.G. Simmons, G.W. Taylor, M.C. Tam, Phys. Rev. B 7 (1973) 3714.
[5] H. Fritzsche, N. Ibaraki, Philos. Mag. B 52 (1985) 299.
[6] B. Gu, Z. Xu, B. Dong, J. Non-Cryst. Solids 97&98 (1987) 479.
[7] S.D. Baranovskii, M. Zhu, T. Faber, F. Hensel, M.B. von der Linden, W.F. van der Weg, Phys. Rev. B 55 (1997) 16226.
[8] A. Rose, Concepts in Photoconductivity and Allied Problems, Robert E. Krieger, New York, 1978, p. 14.
[9] M. Zhu, H. Fritzsche, Philos. Mag. B 53 (1986) 41.
[10] D.S. Misra, A. Kumar, S.C. Agarwal, Phys. Rev. B 31 (1985) 1047.
[11] J.P. Kleider, C. Longeaud, in: Hans Neber-Aeschbacher (Ed.), Hydrogenated Amorphous Silicon, Scitec, Zurich, 1995, p. 597.
[12] R.R. Koropecki, J.A. Schmidt, R. Arce, J. Appl. Phys. 91 (2002) 8965.